Acidification of Morphologically Distinct Endosomes in Mutant and Wild-type Chinese Hamster Ovary Cells

Darrell J. Yamashiro and Frederick R. Maxfield

Department of Pharmacology, New York University School of Medicine, New York 10016

Abstract. In the preceding paper (Yamashiro, D. J., and F. R. Maxfield. 1987. *J. Cell Biol.* 105:2713–2721), we have shown that there is rapid acidification of endosomal compartments to pH 6.3 by 3 min in wild-type Chinese hamster ovary (CHO) cells. In contrast, early acidification of endosomes is markedly reduced in the CHO mutants, DTF 1-5-4 and DTF 1-5-1. Since these CHO mutants are pleiotropically defective in endocytosis (Robbins, A. R., S. S. Peng, and J. L. Marshall. 1983. *J. Cell Biol.* 96:1064–1071; Robbins, A. R., C. Oliver, J. L. Bateman, S. S. Krag, C. J. Galloway, and I. Mellman. 1984. *J. Cell Biol.* 99: 1296–1308), our results are consistent with a requirement for proper acidification of early endocytic compartments in many pH-regulated endocytic processes. In this paper, by measuring the pH of morphologically distinct endosomes using fluorescence microscopy and digital image analysis, we have determined in which of the endocytic compartments the defective acidification occurs. We found that the acidification of both the *para*-Golgi recycling endosomes and lysosomes was normal in the CHO mutants DTG 1-5-4 and DTF 1-5-1. The mean pH of large endosomes containing either fluorescein-labeled α_2-macroglobulin or fluorescein-isothiocyanate dextran was only slightly less acidic in the mutant cells than in wild-type cells. However, when we examined the pH of individual large (150–250 nm) endosomes, we found that there was an increased number of endosomes with a pH >6.5 in the CHO mutants when compared with wild-type cells. Heterogeneity in the acidification of large endosomes was also seen in DTF 1-5-1 by a combined null point pH method and digital image analysis technique. In addition, both CHO mutants showed a marked decrease in the acidification of the earliest endosomal compartment, a diffusely fluorescent compartment comprised of small vesicles and tubules. We suggest that the defect in endosome acidification is most pronounced in the early, small vesicular, and tubular endosomes and that this defect partially carries over to the large endosomes that are involved in the sorting and processing of ligands. The proper step-wise acidification of the different endosomes along the endocytic pathway may have an important role in the regulation of endocytic processes.

In the preceding paper (40) we examined the kinetics of endosome acidification in wild-type and mutant Chinese hamster ovary (CHO) cells. We found in wild-type cells that there was a rapid (3–5 min) acidification of endosomes to pH 6.2–6.3. With time, α_2-macroglobulin (α_2M)[1] and fluorescein-isothiocyanate dextran (F-Dex), molecules that are routed to lysosomes, are found in progressively more acidic endocytic compartments (pH < 6.0), while transferrin (Tf), a ligand that recycles, is found in a more neutral compartment (pH 6.5). Endosomes of the CHO mutants DTG 1-5-4 and DTF 1-5-1 (13, 27, 28) also show differences in pH, along with a marked decrease in early acidification (40). These and other studies on the kinetics of endosome acidification (12, 29, 32) show that endosomes within the same cell can vary in their pH.

Differences in acidification may be important in determining the function of an endocytic compartment, because endocytic processes vary in their acidification requirements. Low density lipoprotein (LDL) and α_2M need only mildly acidic conditions (pH 6.5–6.7) to dissociate from their receptors (1, 17), whereas lysosomal enzyme dissociation (8), iron release (3, 15, 26), and penetration of diphtheria toxin (5, 31) all require a pH of <6.0. Therefore, measuring the pH of a specific type of endosome may help elucidate the role that endocytic compartment has in a particular physiologic process.

From kinetic studies (12, 29, 32, 40) it is not clear whether

Dr. Maxfield's present address is Departments of Pathology and Physiology, College of Physicians and Surgeons, Columbia University, New York, NY 10032.

1. *Abbreviations used in this paper*: α_2M, α_2-macroglobulin; α_2M-gold, α_2-macroglobulin adsorbed to colloidal gold; AA/MA, ammonium acetate/methylamine; F-α_2M, fluorescein-labeled α_2-macroglobulin; F-Dex, fluorescein isothiocyanate dextran; F-Tf, fluorescein-labeled transferrin; LDL, low density lipoprotein; man 6-P, mannose 6-phosphate; R-α_2M, rhodamine-labeled α_2-macroglobulin; Tf, transferrin; WTB, wild-type CHO cells.

progressive acidification results from pH changes within an organelle or from passage among organelles that are regulated to different pH values. Several different types of endosomes have been described in CHO cells (34, 39, 41). These include: (*a*) early, small vesicular and tubular endosomes often located near the cell surface, (*b*) large endosomes with diameters of 150–250 nm, and (*c*) recycling endosomes comprised of small vesicles and tubules located near the Golgi complex. The kinetics of passage through these compartments is not highly synchronous. As early as 5 min some Tf is found in the recycling endosomes and some F-Dex is found in large endosomes. Approximately half of the α_2M-gold is in large endosomes at that time (41). Upon further incubation more F-Dex and α_2M is in large endosomes, and Tf moves into recycling endosomes. The half-time for exocytosis of Tf is ~10 min (19, 41). Delivery of α_2M to lysosomes occurs over a period of 30–60 min (41).[2] That passage between these compartments is asynchronous means that measuring pH only as a function of time will provide an incomplete picture since time-dependent changes in pH may occur from either changes in a single organelle or as a result of passage between organelles.

To measure the pH of specific endocytic compartments we have used fluorescence microscopy and digital image analysis (18, 35, 37). We have previously shown in wild-type CHO cells that the recycling endosomes have a pH of 6.4, while the large endosomes have a pH of 5.2 (41). We have now used digital image analysis to measure the pH of morphologically distinct endosomes in both wild-type and mutant CHO cells. A null point pH method (40) has also enabled us to extend the use of digital image analysis to examine the pH of early endosomes. We found that the pH of the diffusely distributed early endosomes was higher in the mutants than in wild-type cells. The pH of some large vesicular endosomes was also elevated, but the pH of many of these large endosomes was in the normal range (pH 5.0–6.0). The pH of the *para*-Golgi recycling endosomes and lysosomes was essentially the same in the mutant and wild-type cells. Our results suggest that the proper functioning of pH regulatory components in early endosomes is required for normal sorting and processing of ligands and receptors.

Materials and Methods

Cells

Wild-type CHO cells (WTB) and the mutants DTF 1-5-1 and DTG 1-5-4 were grown as described (40).

Ligands

Fluorescein-labeled α_2M (F-α_2M), fluorescein isothiocyanate dextran (F-Dex), and fluorescein-labeled Tf (F-Tf) were prepared as described (40). α_2M was adsorbed to colloidal gold (α_2M-gold) as described (36).

Fluorescence Microscopy and Digital Image Analysis

Fluorescence experiments were conducted on a Leitz Diavert fluorescence microscope system (E. Leitz, Inc., Rockleigh, NJ), which has been previously described in detail (18). The microscope is equipped with interchangeable 450- and 490-nm band pass filters, an image intensification video system, and a Leitz MPV microscope spectrofluorometer. To measure the pH of endocytic compartments cells were incubated with a fluorescein-labeled ligand, rinsed free of unbound ligand, and then reincubated for the times indicated. Cells were then rinsed with medium 1 (NaCl 150 mM, KCl 5 mM, $CaCl_2$ 1 mM, glucose 10 mM, and Hepes 20 mM, pH 7.4), and observed by fluorescence microscopy. Video images of fluorescence at 450- and 490-nm excitation were obtained using either a model 65 MKII SIT camera (Dage-MTI, Inc., Wabash, MI) or a Zeiss-Venus TV3M camera (Carl Zeiss, Inc., Thornwood, NY) and recorded on a Panasonic NV 8030 videotape recorder. Video output from the recorder was passed through a model CCDHPS time base corrector (Fortel Inc., Norcross, GA), and images were digitized on a model IP8500 image processor (Gould, Inc., San Jose, CA), with a MicroVAX II (Digital Equipment Corp., Marlboro, MA) as host computer. Digitized images were further processed as described (10, 18, 37, 41). Briefly, 490- and 450-nm images were divided into 64 pixel × 64 pixel regions (13.4 μm × 13.4 μm), and the background fluorescence (defined as the median [50th percentile] intensity of the region) was subtracted from each pixel. To identify structures corresponding to the indicated endocytic compartment, a threshold value was chosen from the 490-nm background corrected image (10). The pixels above this intensity were used for the intensity measurements. The intensity of the corresponding pixels of the 450-nm background corrected image were then used to calculate the I_{450}/I_{490} ratio. pH values were assigned by comparison of the I_{450}/I_{490} to a pH calibration curve as described previously (18, 37, 39). With our microscope system, as configured for these experiments, the I_{450}/I_{490} ratio is ~1.3 at pH 5, and falls to 0.4 at pH 7. This procedure has been extensively tested (18, 37, 41) and provides a method for measuring vesicle pH against a diffuse background. In-cell calibration curves were made using the same incubations as for the experiments, and pH values agree with the solution calibration curves to ±0.2 pH units over the range 5.0–6.8. Although the definition of vesicles is somewhat arbitrary (due to threshold), pH is not affected by this since exactly the same pixels are used in the 490- and 450-nm images (18, 37). In all cases, the intensity response of the video system was monitored, and appropriate corrections for nonlinearity were made when necessary.

The acidification of punctate and diffuse endocytic compartments was examined by a null point method similar to that described for whole cell measurements (40) except that video images were recorded instead of photometric measurements of fluorescence intensity. To quantify the changes in fluorescence intensity that occurred after the addition of ammonium acetate/methylamine (AA/MA), images were digitized and the fluorescence intensities of corresponding areas were determined. For the diffuse endocytic compartment 10 × 10 pixel (2.1 × 2.1 μm) areas were measured, and for the punctate endocytic compartment 4 × 4 pixel (0.84 × 0.84 μm) areas. The percent change in intensity for each area was then calculated.

Electron Microscopy and Acid Phosphatase Cytochemistry

Cells were incubated with α_2M-gold as specified in the text. Cells were then fixed in 1% glutaraldehyde, 2% paraformaldehyde in 0.1 M sodium cacodylate, pH 7.4 for 30 min at 23°C. Cells were rinsed in 0.1 M sodium cacodylate containing 7% sucrose, pH 7.4, and stored overnight in the same buffer. To stain for acid phosphatase, cells were rinsed in 50 mM sodium acetate, 7% sucrose, pH 5.0 (acetate buffer), and then incubated with 10 mM β-glycerolphosphate and 1 mg/ml lead nitrate in acetate buffer for 1 h at 34°C. Cells were rinsed with acetate buffer and postfixed in 1% OsO_4 reduced with 1% potassium ferrocyanide in 0.1 M sodium cacodylate pH 7.4 for 1 h at 4°C. Samples were rinsed with water, dehydrated by passage through graded ethanols, and embedded in the culture dish with EPON resin (SPI Supplies, West Chester, PA). Thin sections were cut using a Sorvall MT5000 microtome (DuPont Instruments, Newtown, CT), counterstained with uranyl acetate, and observed with either a Jeol 100S or a Phillips 301 electron microscope operated at 80 kV.

To measure total cell acid phosphatase, cells grown in 75-cm^2 flasks were removed by trypsinization and then pelleted in McCoy's 5A medium containing 5% FBS. Cells were then rinsed, pelleted, and resuspended in hypoosmotic buffer (Hepes 10 mM, pH 7.4). Cells were broken open by freezing and thawing, and then sonicated in hypoosmotic buffer containing 0.2% Triton X-100. Acid phosphatase activity was measured as described, using 4-nitrophenyl phosphate as substrate (21).

Results

To measure the pH of morphologically distinct endocytic compartments we used the pH-dependent properties of fluorescein and image-intensified fluorescence microscopy

2. Yamashiro, D. J., and F. R. Maxfield. Manuscript in preparation.

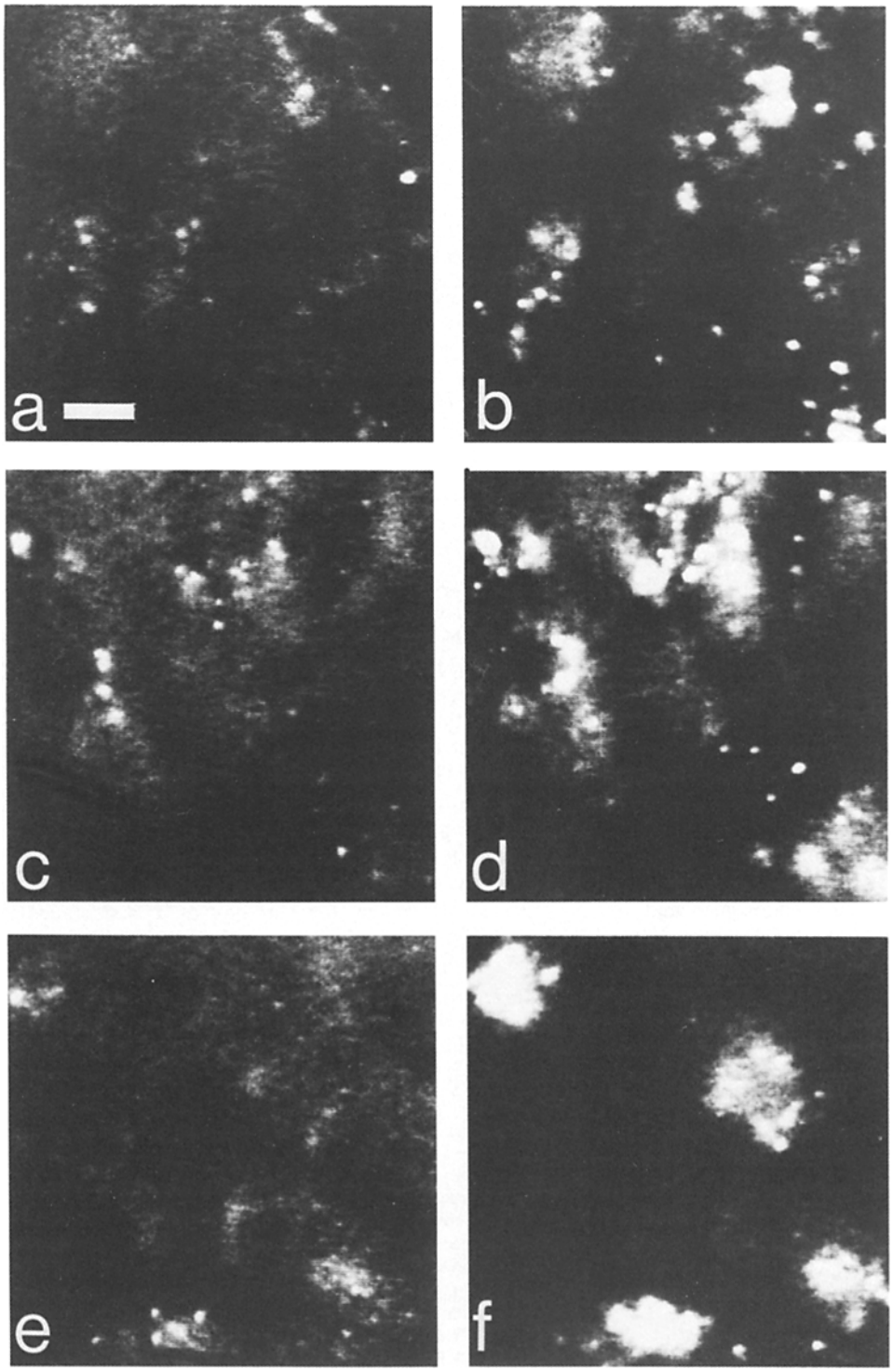

Figure 1. Acidification of large endosomes containing F-α_2M. Cells were incubated with F-α_2M (150 μg/ml) for 15 min at 34°C, and then rinsed with medium 1. WTB (*a*), DTG 1-5-4 (*c*), and DTF 1-5-1 (*e*) cells were observed at 490-nm excitation. The ionophore monensin (10 μM) was added to dissipate the pH gradient, and WTB (*b*), DTG 1-5-4 (*d*), and DTF 1-5-1 (*f*) cells were observed 2 min later. Images were obtained with a Zeiss-Venus TV3M image intensifier camera, videotaped, and digitized on the Gould IP8500. The images were redisplayed on a high resolution monitor and photographed. Bar, 8 μm.

combined with digital image analysis (18, 35, 37). Fluorescein excitation at 490 nm is highly pH dependent, with fluorescence intensity increasing as pH increases from 5 to 7. Since fluorescein fluorescence at 450-nm excitation rises less sharply between pH 5 and 7, a pH calibration curve can be constructed from the ratio of fluorescence intensities at the two excitation wavelengths (I_{450}/I_{490}). With digital image analysis we can subtract the fluorescence contributed by cellular autofluorescence and cell surface fluorescein from our measurements. Individual bright spots corresponding to single large endosomes or a collection of small vesicles and tubules (e.g., the *para*-Golgi recycling endosomes [41]), can be identified by light microscopy, and the pH is calculated from the I_{450}/I_{490}.

pH of Endosomes Containing F-α_2M

We first examined the pH of large endosomes containing F-α_2M. Cells were incubated with F-α_2M for 15 min, rinsed free of ligand, reincubated for 2 min, and then ob-

Table I. pH of Endosomes by Digital Image Analysis

Ligand	Condition	pH		
		WTB	DTG 1-5-4	DTF 1-5-1
F-α_2M	15 min/2 min	5.2 ± 0.1 (n = 179)*	5.7 ± 0.1 (n = 121)	5.6 ± 0.1 (n = 171)
	+ Methylamine	>7.0 (n = 198)	nd	>7.0 (n = 124)
F-Dex	5 min/5 min	5.8 ± 0.1 (n = 116)	6.0 ± 0.1 (n = 106)	6.0 ± 0.1 (n = 103)
	15 min/30–45 min	5.2 ± 0.1 (n = 164)	5.2 ± 0.1 (n = 160)	5.3 ± 0.1 (n = 139)
F-Tf	18 min/2 min	6.4 ± 0.1 (n = 69)‡	6.3 ± 0.1 (n = 40)	6.4 ± 0.1 (n = 51)

Cells were incubated with F-α_2M (150 μg/ml), F-Dex (5 mg/ml), or F-Tf (100 μg/ml) in McCoy's 5A medium containing Hepes (20 mM) and either BSA or ovalbumin (1 mg/ml) at 34°C for the times indicated and then rinsed with medium and reincubated. The cells were placed in medium 1 and the pH of the fluorescein containing structures determined by digital image analysis as described in the Materials and Methods section. For α_2M and F-Dex these structures are primarily large endosomes. For F-Tf the structures are *para*-Golgi recycling endosomes. The pH values are the mean ± standard error of the mean of 3–12 fields of cells. For F-α_2M, methylamine (40 mM) was added at the end of the experiments and the pH measured. nd, not determined.

* Values in parentheses indicate the number of vesicles or discrete structures from which the pH was determined.

‡ The data on pH of F-Tf in WTB cells have been published previously in Yamashiro et al. (41).

served by fluorescence microscopy. F-α_2M was found in a punctate pattern in both wild-type and mutant cells (Fig. 1). As described below, the majority of these structures were large nonlysosomal endosomes. To ascertain whether these large endosomes were acidic, we observed the fluorescence intensity at 490-nm excitation (Fig. 1, *a*, *c*, and *e*). After the addition of monensin, there was a marked increase in the fluorescence intensity of the large endosomes in both the wild-type and mutant cells (Fig. 1, *b*, *d*, and *f*), indicating that these endosomes were acidic in all three cell types.

To quantify the pH of these large endosomes, we used digital image analysis and fluorescence images obtained at 490- and 450-nm excitation. The I_{450}/I_{490} of the vesicles was calculated, and a mean pH value was determined from a pH calibration curve. We found that the large endosomes acidified to average pH values below 6.0 in both DTG 1-5-4 (pH 5.7) and DTF 1-5-1 (pH 5.6, Table I). The large endosomes in wild-type cells were slightly more acidic, with an average pH 5.2. Addition of the weak base methylamine (17, 25) collapsed the endosomal pH gradient (pH > 7.0, Table I).

Intracellular Localization of α_2M

To interpret the fluorescence measurements it was necessary to characterize the α_2M-containing structures by electron microscopy and cytochemistry. To determine the prelysosomal character of the endosomes we used acid phosphatase cytochemistry. Acid phosphatase in contrast to other acid hydrolases is not deficient in I-cell fibroblasts, suggesting that this enzyme is not routed to lysosomes via the mannose-6-phosphate (man-6-P) receptor (14). Use of a lysosomal enzyme that is not carried by the man-6-P receptor was necessary since those enzymes are decreased in the CHO mutants (27, 28). We confirmed that acid phosphatase is not depleted in the mutant cells by measuring the total cell enzyme levels. Using 4-nitrophenyl phosphate as substrate, we found that acid phosphatase levels were actually elevated in the mutants DTG 1-5-4 (141% of WTB, normalized per cell) and DTF 1-5-1 (174% of WTB), indicating that this enzyme is a valid marker for lysosomes in the CHO mutants.

For electron microscopy, we incubated cells with α_2M-gold and stained the cells for acid phosphatase using β-glycerolphosphate as substrate. We optimized the acid phosphatase staining, so that lysosomes were heavily labeled but there was little nonspecific staining in the cytoplasm and nucleus. After 15 min of endocytosis, the majority of α_2M-gold in the wild-type and mutant cells was in large, acid phosphatase negative endosomes (Table II). About 15–21% of the α_2M-gold was in small vesicular and tubular endosomes (diameter <120 nm), often located near the cell surface (Fig. 2 *a*). Less than 10% of the α_2M-gold was in lysosomes (Fig. 2 *b*) at this time (Table II). Large endosomes and lysosomes would both appear as bright dots by fluorescence microscopy. The electron microscopic cytochemistry demonstrates that only ~10% of the large vesicles contain detectable acid phosphatase at the time of our pH measurements with F-α_2M. An endosomal localization was also supported by studies on the degradation of ^{125}I-α_2M. We have previously shown that <10% of α_2M is degraded in WTB cells after a 10-min incubation and 10-min chase (41).

With a 10-min pulse and a 35-min chase, 26% of the α_2M-gold in DTF 1-5-1 and 17% in DTG 1-5-4 was in lysosomes (Table II). These data and biochemical analysis of the internalization and degradation of α_2M (footnote 2) demonstrate that the endocytosis pathway of α_2M is not severely altered in the mutant cells.

Table II. Intracellular Distribution of α_2M-Gold

Cells	Condition	% Distribution of α_2M-Gold*			
		SV/T	Large endosome	Lysosome	Particles
WTB	10 min/5 min	19	73	8	n = 799
	10 min/35 min	8	65	27	n = 590
DTG 1-5-4	10 min/5 min	21	74	5	n = 732
	10 min/35 min	11	72	17	n = 816
DTF 1-5-1	10 min/5 min	15	77	8	n = 661
	10 min/35 min	3	71	26	n = 431

Cells were incubated with α_2M-gold (10 μg/ml equivalent α_2M) in McCoy's 5A medium containing Hepes (20 mM) and BSA (1 mg/ml) for 10 min at 34°C. Cells were then rinsed with medium and reincubated for either 5 or 35 min. Cells were fixed and processed for acid phosphatase cytochemistry and electron microscopy as described in the Materials and Methods section.

*α_2M-gold containing structures were categorized as SV/T (small vesicle/tubular endosome, diameter <0.12 μm), large endosome (diameter >0.12 μm), or lysosome (acid phosphatase positive). Particles were counted either from electron micrographs or directly from the viewing screen.

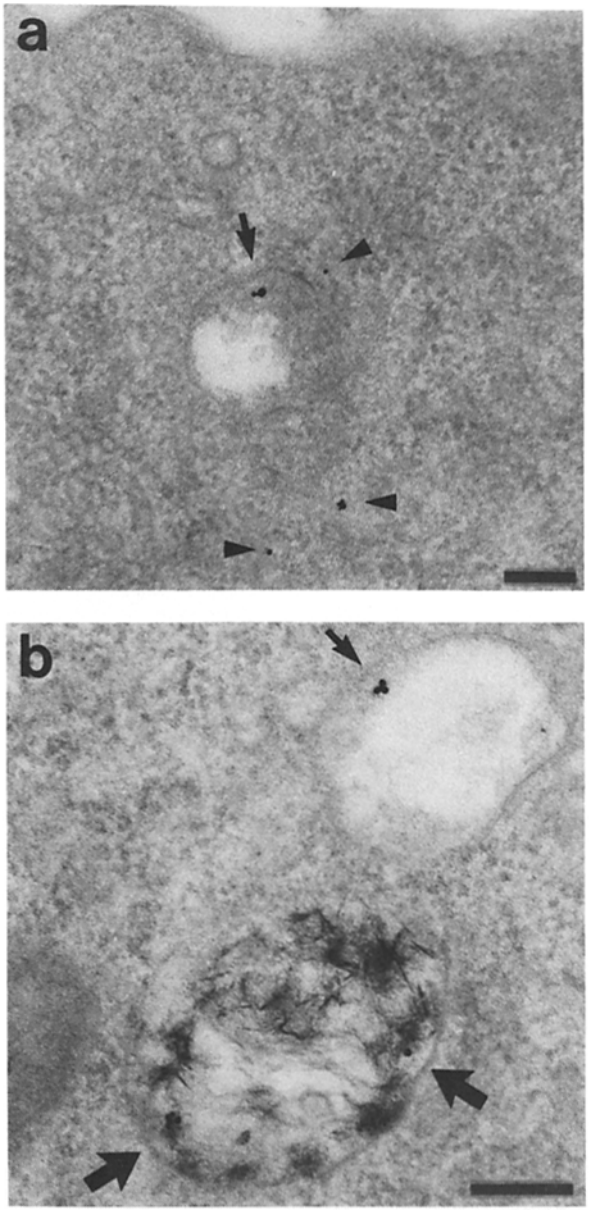

Figure 2. Ultrastructural localization of α_2M-gold. DTG 1-5-4 and DTF 1-5-1 cells were incubated with α_2M-gold (10 μg/ml equivalent α_2M) in McCoy's 5A medium containing Hepes (20 mM) and BSA (1 mg/ml) for 10 min at 34°C. Cells were then rinsed with medium and reincubated for 5 min. Cells were fixed and processed for acid phosphatase cytochemistry and electron microscopy as described in the Materials and Methods section. In DTG 1-5-4 (*a*) the arrowheads indicate α_2M-gold in a small vesicle/tubular endosome, and a small arrow indicates α_2M-gold in a large endosome. In DTF 1-5-1 (*b*) arrows indicate the location of α_2M-gold in a large endosome (*small arrow*) and in an acid phosphatase positive lysosome (*large arrow*). The colloidal gold particles can be seen easily over the background of the acid phosphatase reaction product. Bar, 0.2 μm.

Endocytosis of Tf

In wild-type cells Tf rapidly segregates from α_2M and enters recycling endosomes of pH 6.4 located near the Golgi complex (41). This segregation becomes observable within 5 min. Essentially identical sorting of F-Tf from R-α_2M was observed in the mutant and wild-type cell lines when examined by fluorescence microscopy (data not shown). We measured the pH of the F-Tf *para*-Golgi recycling endosomes by digital image analysis. The pH of these endosomes in DTG 1-5-4 and DTF 1-5-1 (pH 6.3–6.4) was similar to that of wild-type cells (Table I), indicating that acidification of the recycling endosomes was not affected in the mutants.

pH of Endosomes and Lysosomes Containing F-Dex

We also measured the pH of large endosomes and lysosomes containing the fluid phase marker F-Dex (Table I). Cells were incubated with F-Dex for 5 min, rinsed, and reincubated for 5 min. The mean pH of endosomes identified by our image processing method at this time was pH 5.8 in WTB, pH 6.0 in DTG 1-5-4, and pH 6.0 in DTF 1-5-1. This population of vesicles is endosomal, since after 10 min of endocytosis, the vast majority of F-Dex was in a light density endosomal fraction after Percoll density centrifugation (28). The pH of lysosomes was also determined by incubating cells with F-Dex for 10 min, and then reincubated for 30–45 min. We found that lysosomes in the mutants and WTB had similar mean pH values of 5.2–5.3.

Although the mean pH of endosomes containing F-Dex is nearly the same in the mutant and wild-type cells, the distribution of pH values of individual large endosomes is more heterogeneous in the mutant cells. Fig. 3 (*left*) shows the pH histograms of large endosomes labeled with F-Dex for 5 min, and reincubated for 5 min (these endosomes were used to compute the average pH in Table I). For comparison, the standard deviation of pH of individual endosomes in fixed cells equilibrated to pH 6.0 is 0.3 pH units. The distribution of endosomal pH was essentially unimodal in WTB, with a population of endosomes having a pH centered near 5.6. There were, however, a significant number of endosomes in wild-type cells with pH values above 6.5. In DTF 1-5-1, the distribution of endosomal pH was clearly bimodal, with one group having a pH near 5.6 and the second group having a pH near 7.0. In DTG 1-5-4, the pH of endosomes had a heterogeneous distribution.

Distribution of lysosomal pH was similar in wild-type and mutant cells, having a unimodal distribution centered around a pH value of ~5.2 (Fig. 3, *right*). These results indicate that there is a defect in the acidification of a population of large endosomes in the mutant DTF 1-5-1 and to a lesser extent in DTG 1-5-4. The mutants, however, still have a large population of large endosomes that acidify to values below pH 6.

Acidification of Diffuse and Punctate Endocytic Compartments

In our studies of the kinetics of acidification based on photometry measurements of whole cells, we found that acidification of endosomes containing F-Dex after a 5-min incubation and 5-min chase was significantly altered in the mutant cell lines (40). As shown here, the mean pH of the large endosomes at that time is only slightly more alkaline in the mutants. This suggested that the altered pH might be more pronounced in endosomes such as the early small vesicle and tubules, which would not appear as discrete vesicles by fluorescence microscopy. To test this directly, we combined the null point method described in the preceding paper (40) with digital image analysis to separately measure the pH

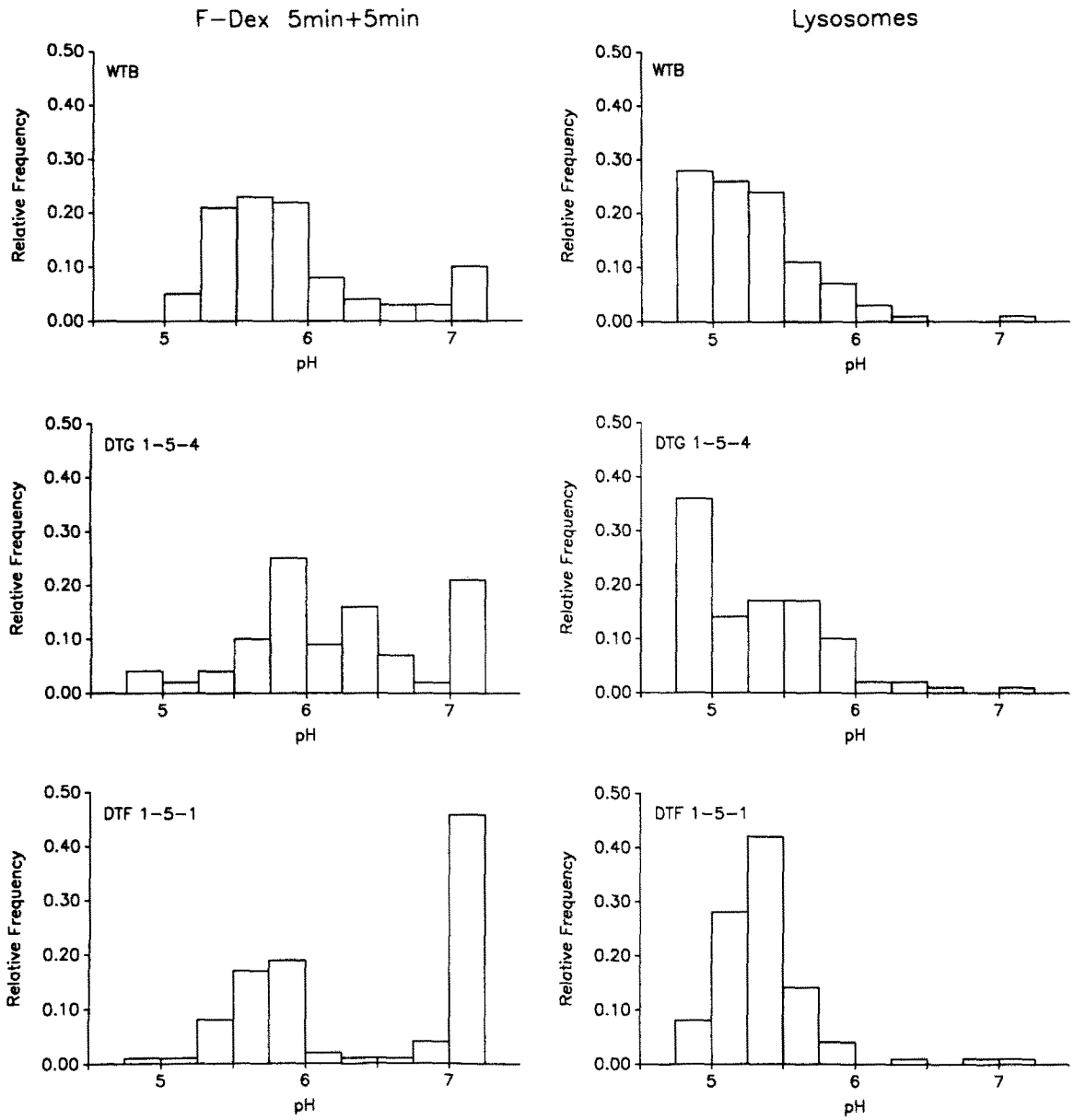

Figure 3. pH histogram of large endosomes and lysosomes containing F-Dex. The endosomes and lysosomes used to compute the mean pH shown in Table I were analyzed individually. The I_{450}/I_{490} of individual vesicles was calculated and the pH determined by comparison to an in cell calibration curve as described in Materials and Methods. Endosomes were grouped into pH bins of 0.25 pH units. The upper and lower bins contain endosomes with I_{450}/I_{490} corresponding to pH >7.0 and pH <5.0, respectively. (See Table I, F-Dex data, for number of vesicles.) To estimate the error of an individual pH measurement, cells were fixed, and placed in a buffer of known pH. The standard deviation of the I_{450}/I_{490} values in these fixed cells corresponds to a pH range of ± 0.3 pH units.

in endosomes giving diffuse fluorescence (i.e., early endosomes) and endosomes giving punctate fluorescence (i.e., large endosomes). The null point method determines average pH by lowering the pH of the extracellular medium using a nonpermeant buffer and then equilibrating the pH of the intracellular compartments with the external (test) pH by using a weak base/weak acid mixture such as AA/MA. If the pH of the intracellular compartment is below the test pH, then the fluorescence intensity at 490-nm excitation will increase upon addition of AA/MA.

Cells were incubated with F-Dex for 5 min, rinsed free of ligand, and then reincubated for 1 min. The cells were then cooled, the external pH lowered to pH 6.4, and the cells observed by fluorescence microscopy (Fig. 4, *a*, *c*, and *e*). After the addition of AA/MA at pH 6.4, there was an increase in the fluorescence intensity of many large endosomes in all three cell lines (Fig. 4, *b*, *d*, and *f*), demonstrating that these endosomes had a pH <6.4. When we determined the change in the fluorescence intensity of the entire field, so that all the intracellular compartments were included, we found for WTB that the fluorescence increased (+4.1%), indicating that the average pH was <6.4. For both DTG 1-5-4 and DTF 1-5-1, we found that the fluorescence intensity decreased (−7.3% and −3.4%, respectively) after the addition of AA/

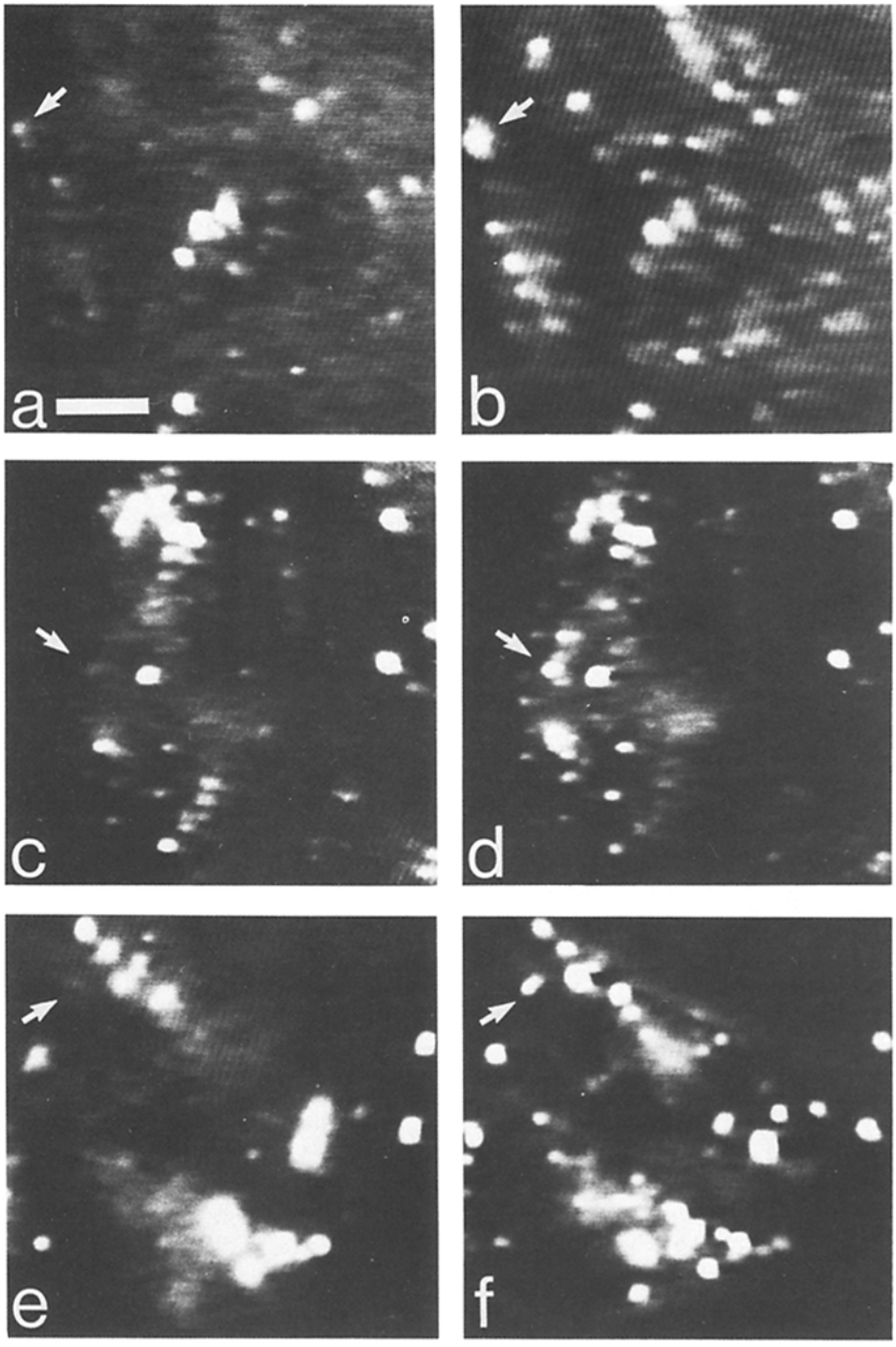

Figure 4. Acidification of punctate and diffuse structures using the null point method. Cells were incubated with F-Dex for 5 min, rinsed, and reincubated for 1 min. The external pH was lowered to pH 6.4 as described in Materials and Methods. The fluorescence intensity at 490-nm excitation was observed for WTB (*a*), DTG 1-5-4 (*c*), and DTF 1-5-1 (*e*). AA/MA was then added to equilibrate the pH of the intracellular compartment with the external pH and the fluorescence intensity of WTB (*b*), DTG 1-5-4 (*d*), and DTF 1-5-1 (*f*) was observed after 90 s. Arrows indicate vesicles that increased in intensity after addition of AA/MA, demonstrating that the pH of the vesicles was <pH 6.4. Bar, 4 μm.

MA, indicating that the average pH was >6.4. These results agree with our previous results from whole cell photometry measurements, where we found that the average pH of the endocytic compartments at this time was pH 6.2 for WTB and pH 6.7 for both DTG 1-5-4 and DTF 1-5-1 (40).

To quantify the changes in the fluorescence intensity of the punctate endocytic compartments and the diffuse endocytic compartments, we determined the average fluorescence intensity of 2 μm × 2 μm areas for diffusely fluorescent regions lacking any detectable punctate fluorescence and 0.8 μm × 0.8 μm areas centered on bright dots of bright dots of fluorescence. We then determined the change in the fluorescence intensity for both the diffuse and punctate areas after the addition of AA/MA. These results are shown as a histogram (Fig. 5). The addition of AA/MA caused an increase in the fluorescence intensity in the majority of punctate structures for WTB (74% of vesicles) and DTG 1-5-4 (64%). In DTF 1-5-1, many of the dots decreased in fluorescence intensity (55%), indicating that approximately half of these large endosomes had a pH >6.4. These results support

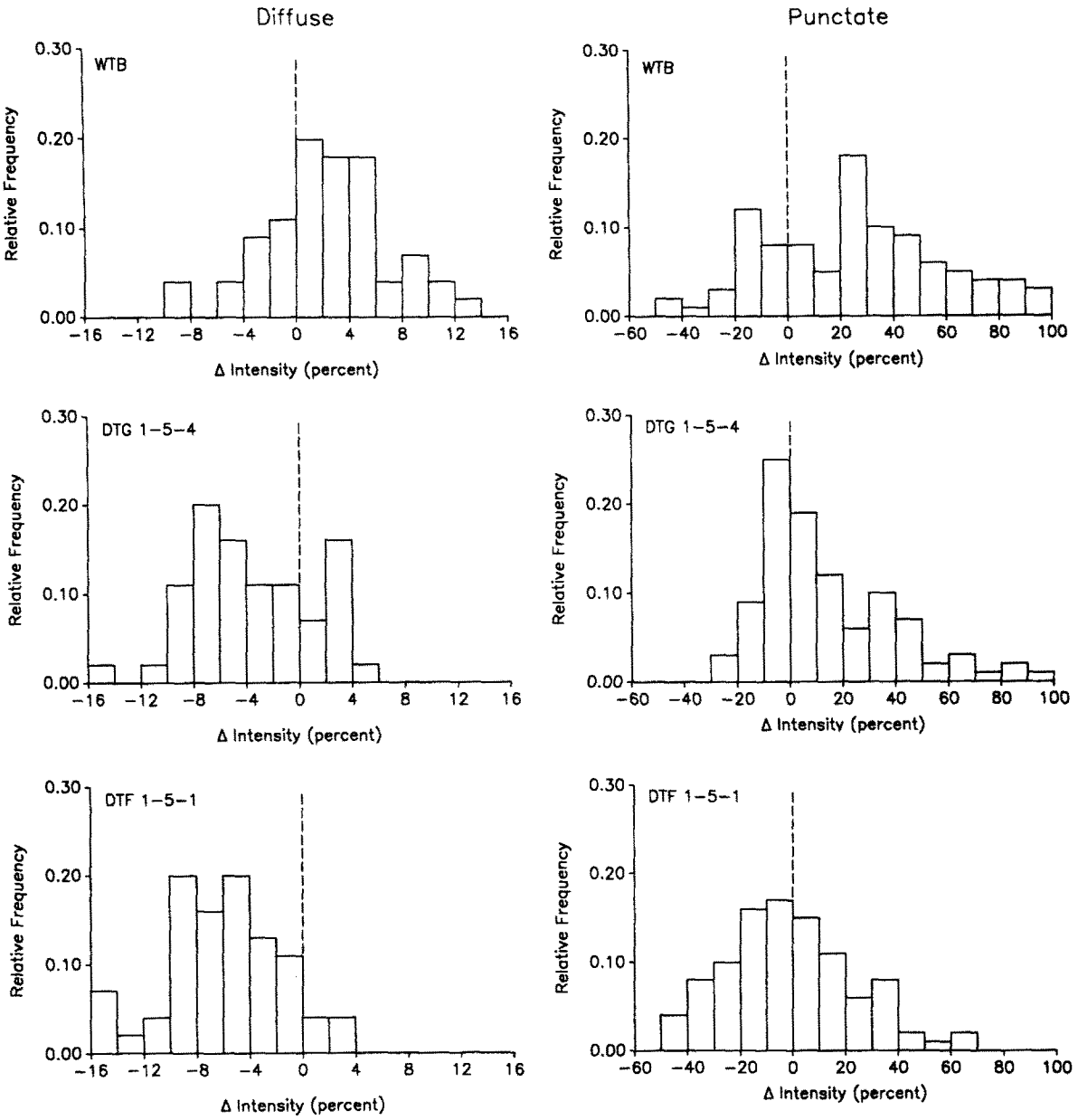

Figure 5. Histogram of punctate and diffuse endocytic compartments. The change in fluorescence intensity of diffuse and punctate areas was determined as described in Materials and Methods. Cells were incubated with F-Dex for 5 min, rinsed, and reincubated for 1 min. The test pH was pH 6.4. Those areas whose pH was below pH 6.4 have a positive Δintensity, while those areas whose pH was above pH 6.4 have a negative Δintensity. A total of 100 punctate areas and 45 diffuse areas were measured from two separate experiments.

our finding from the pH histogram of individual endosomes (Fig. 3), that DTF 1-5-1 has a defect in the acidification of some of its large endosomes.

There was a marked difference in the acidification of the diffusely fluorescent endocytic compartment. For WTB, the majority of the diffuse areas increased in fluorescence intensity (73%), indicating that the pH of the diffuse compartment is also below pH 6.4. However, for both DTG 1-5-4 and DTF 1-5-1, the majority of the diffuse areas decreased in fluorescence intensity (76% and 91%, respectively), indicating that the pH of the diffuse compartment is >pH 6.4. These results demonstrate that a major component of the reduced acidification seen in the mutants is due to altered acidification of early endosomes. The alteration in these early small vesicle and tubule endosomes is much more pronounced than in the large endosomes. Even at early times (e.g., 5-min incubation, 1-min chase) many of the endosomes in both mutant cell lines have a pH <6.4 (Fig. 5).

Discussion

After endocytosis via coated pits, molecules pass through a series of endocytic compartments and are either recycled to the cell surface or delivered to lysosomes for degradation. In CHO cells several distinct organelles can be identified by light and electron microscopy. At early times α_2M-gold and Tf-ferritin are found in small vesicles and tubules near the surface (41). These are shown schematically as "early endo-

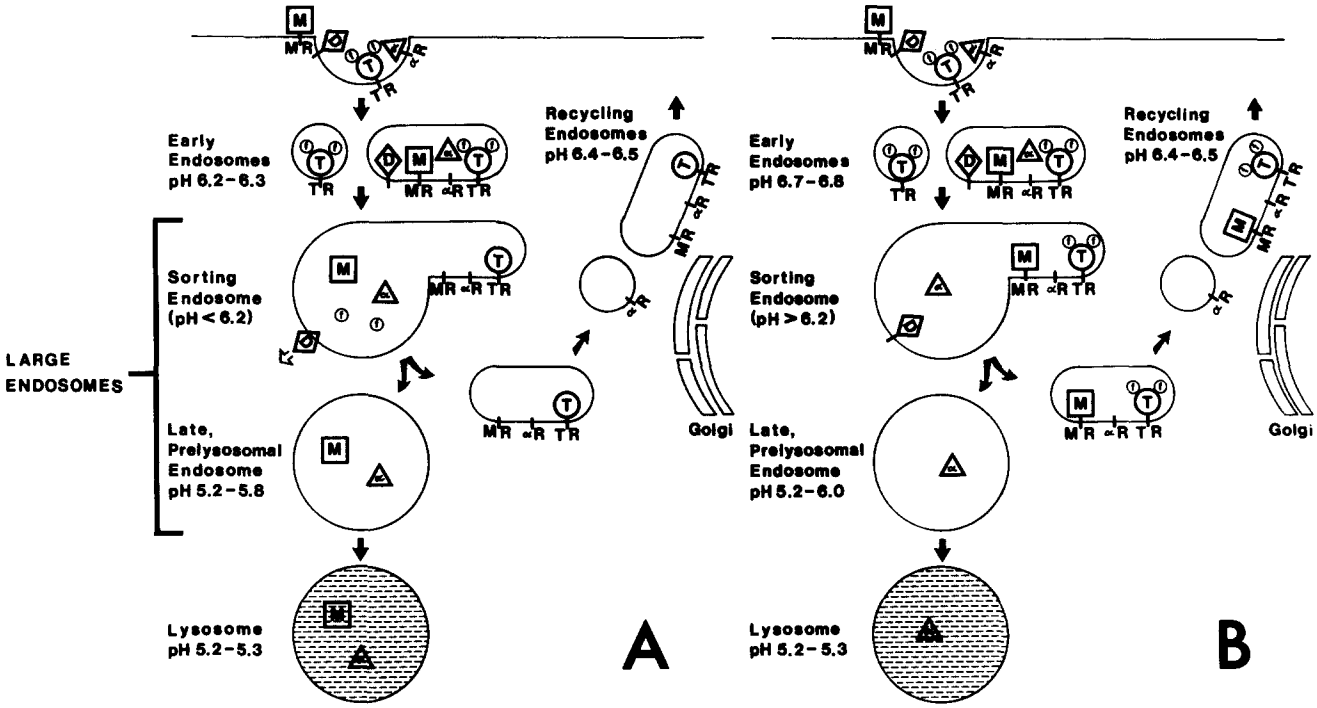

Figure 6. Models of the endocytic pathways in wild-type and mutant CHO cells. These are working models of the endocytic pathways found in wild-type cells (*A*) and in the CHO mutants DTG 1-5-4 and DTF 1-5-1 (*B*). Enzymes bearing man 6-P (*M*) bound to the man 6-P receptor (*MR*), diphtheria toxin (*D*), diferric (*f*) transferrin (*T*) bound to the transferrin receptor (*TR*), and α_2M (α) to the α_2M receptor (αR) are internalized through coated pits into small vesicular and tubular "early endosomes." The pH of the early endosomes is pH 6.2–6.3 in the wild-type cells and pH 6.7–6.8 in the CHO mutants. Early endosomes are sufficiently acidic to dissociate α_2M from its receptor. The ligands and their receptors move to a large vesicle, with tubular extensions, termed "sorting endosomes." The sorting endosome has a pH below 6.2 in wild-type cells and a pH >6.2 in the mutants. The sorting endosome in the wild-type cells, but not the mutants, is the site where man 6-P ligands dissociate from their receptors, iron is released from transferrin, and diphtheria toxin penetrates into the cytosol. Apotransferrin bound to its receptor, and the receptors for both α_2M and man 6-P ligands recycle back to the cell surface via "recycling endosomes" found near the Golgi complex. The dissociated man 6-P ligand and α_2M move to late, prelysosomal endosomes, and finally to lysosomes. In the CHO mutants, man 6-P bound to its receptor, diferric transferrin, and α_2M receptors recycle back to the cell surface. Only α_2M moves to late, prelysosomal endosomes and is then degraded in lysosomes.

somes" in Fig. 6. These vesicles are not observable as discrete structures in our fluorescence experiments; they appear as diffusely distributed fluorescence. Within a few minutes some Tf-ferritin and most of the α_2M-gold appears in "large endosomes" with diameters of 150–250 nm (41). These large endosomes are visible as discrete bright dots in our fluorescence microscopy experiments. In the schematic diagram in Fig. 6, two types of large endosomes are shown. The "sorting endosomes" contain recycling membrane components that are absent from the "late, prelysosomal endosomes." The late prelysosomal endosomes are observable by fluorescence microscopy as structures containing R-α_2M after segregation from F-Tf (41).

With further time of incubation, most of the α_2M-gold is delivered to lysosomes, and Tf-ferritin accumulates in small vesicles and tubules (recycling endosomes) near the Golgi complex before release to the cell surface (41). By fluorescence microscopy the lysosomes are not distinguishable from large endosomes. The recycling endosomes in CHO cells are observed by fluorescence microscopy as a cloud of fluorescence near the nucleus, which is not resolvable into the individual vesicles. The juxtanuclear concentration distinguishes the recycling endosomes from the early endosomes. This has allowed us to separately measure the pH of recycling endosomes in CHO cells by digital image analysis (41; Table I).

The names we have assigned to the various endosomes are based on our current understanding of the different endocytic pathways in CHO cells. The endosomes that we describe are similar, if not identical, to those previously identified in other cell types (2, 9, 24, 33). Early endosomes have also been termed "peripheral endosomes" due to their frequent localization near the cell surface. Large endosomes is a broad category and includes endosomes termed "endocytic vesicles," "receptosomes," "late endosomes," "internal endosomes," and "multivesicular endosomes." The sorting endosome is essentially the CURL (compartment of uncoupling receptor and ligand) described by Geuze et al. (6) in hepatoma cells. Like CURL, the tubular extensions of the sorting endosome (Fig. 6) could concentrate the recycling receptors in a low volume/high surface area compartment and thus exclude luminal ligand (6, 7). The late, prelysosomal endosomes is the last organelle before lysosomes, and lacks recycling elements and would correspond to receptor-negative endosomes (22).

Based on the pH measurements reported in this paper and our previous papers (40, 41) pH values have been assigned to these organelles as shown in Fig. 6. At very early times

(i.e., 3–5 min) the average pH of F-Dex or F-Tf containing compartments is 6.2–6.3 (40), and the pH of diffusely fluorescent endosomes containing F-Dex is <6.4 (Fig. 5). Thus, we assign a pH of 6.2–6.3 to the early endosomes. The pH of large endosomes containing F-α_2M or F-Dex at late times is in the range from 5.2–5.8 under various conditions (Table I), and we have assigned this pH to the late, prelysosomal endosomes. There are no separate pH measurements on well defined sorting endosomes. From the increase in vesicle brightness when equilibrated to pH 6.4 (Fig. 4, *a* and *b*, and 5) it is clear that most large endosomes are well below pH 6.4 as early as 5 min. Furthermore, a pH of 6.2 or below would be required for such functions as removing iron from Tf (3, 15, 26) and dissociating lysosomal enzymes from man-6-P receptors (8). Based on this, we have assigned a pH of <6.2 to the sorting endosome. Further work will be required to specifically measure the pH of this compartment. The pH of recycling endosomes is based on a previous study using F-Tf (41), and the lysosomal pH is determined from long incubation with F-Dex (Table I).

The most clear cut change in endosomal pH in the mutant cell lines is in the early endosomes. Based on whole cell measurements (40) and measurements of diffusely fluorescent structures at early times (Fig. 5), we conclude that the pH of early endosomes in both mutants is ~6.7–6.8. In contrast, the acidification of recycling endosomes and lysosomes is normal in the mutants. The pH of large endosomes in the mutants is more complex. On the average, the pH of the large endosomes is slightly less acidic in the mutants than in the wild-type cells (Table I). More striking is the heterogeneity in the pH of these endosomes in the mutants (Fig. 3). We speculate that the higher pH large endosomes are the sorting endosomes; this would be consistent with the inefficiency of the cells in releasing iron from Tf (13, 40) and in delivering endocytosed lysosomal enzymes to lysosomes (27, 28). Based on this we assign a pH >6.2 to the sorting endosomes and a pH of 5.2–6.0 to the late prelysosomal endosomes in the mutants.

Based on the pH values for the various endosomes we can suggest specific roles for each compartment in endocytic processes. In wild-type cells, the pH of 6.2 found in the early endosomes could allow the dissociation of both α_2M and LDL to occur while inside that organelle. Subsequent fusion of an early endosome with a sorting endosome would transfer luminal contents and membrane components to an organelle that could segregate the recycling receptors from the ligands destined for lysosomes. Studies in hepatocytes have shown that dissociation of asialoglycoproteins from its receptor is a discrete event that precedes segregation (38). Ligands that require a more acidic pH to dissociate from their receptor (e.g., lysosomal enzymes) might uncouple in later, more acidic compartments. Thus, whether a compartment functions in the uncoupling of a ligand from a receptor would depend on the pH sensitivity of the particular ligand.

The altered endosomal pH pattern in the mutants is consistent with many of their properties. A pH >6.2 in early endosomes and sorting endosomes is in agreement with the failure to release iron from Tf and inability to release endocytosed lysosomal enzymes since both processes require a pH <6.0. On the other hand, the pH in the sorting endosomes, and possibly the early endosomes as well, is sufficiently low to release α_2M and LDL from their receptors (1, 17). This allows these ligands to be delivered normally to lysosomes in DTG 1-5-4 and DTF 1-5-1 (27; Table II).[2] Similar results have been found with temperature-sensitive, endocytosis CHO mutants from the same complementation groups (30).

The decreased sensitivity of the mutant cells to diphtheria toxin may be partially attributed to the defect in acidification of either early or sorting endosomes, suggesting that penetration may occur from one of those organelles. However, since the bulk of toxin is degraded in lysosomes (4), exposure to the acidic pH of late, prelysosomal endosomes is apparently not sufficient to cause penetration of the toxin into the cytoplasm. Recent evidence has suggested that acidification is required for processing of the toxin and insertion into the membrane, but that entry into the cytosol is acid-independent (11). Other factors may be involved in determining the sensitivity of a cell to diphtheria toxin (23). Thus, the resistance of the mutants to diphtheria toxin could in part be determined by other characteristics of the cells in addition to the alterations in pH.

Penetration of Semliki Forest virus requires exposure to a pH of 6.2 or below and occurs after a lag of a few minutes after internalization in various cell types (12, 16). This is consistent with penetration occurring from large endosomes. The resistance of the mutant cell lines to enveloped viruses (27, 28) would appear to be in conflict with our finding that many of the large endosomes in the mutants have a pH <6.2. However, studies of the kinetics of Semliki Forest virus uncoating and penetration have shown that these processes are very similar in the mutants and wild-type cells (Marsh, M., A. Helenius, and I. Mellman, personal communication). This is consistent with our pH measurements and indicates that the virus resistance occurs at another step of the infection.

Our finding that the primary acidification defect in the mutants resides in early endosomes provides important information regarding mechanisms of pH regulation. It is clear that early and late prelysosomal endosomes are regulated to different pH values by distinct mechanisms. In addition, our finding that the pH of the *para*-Golgi recycling endosomes is not only less acidic than the large endosomes but also unaltered in the mutants, indicates that there may be a third pH regulatory mechanism for the recycling pathway. Our work also suggests that early endosomes and some large endosomes share part of their acidification mechanism, since defective acidification of early endosomes carries over to some large endosomes. At present it is not known how the different endocytic compartments are regulated to different pH values (20).

Our work with both the mutant and wild-type CHO cells illustrates the complexity and importance of early and late endosomal acidification. Further effort will be required to fully understand the consequence of this stepwise acidification and to isolate the mechanisms involved in pH regulation of the various compartments.

We thank Ms. Sharon Fluss, Ms. Ann Ryan, Mr. Peter Peirce, and Mr. John Alves for technical assistance, and Ms. Kristy Brown and Dr. Ivan Ivanov for assistance with the electron microscopy studies. We are grateful to Dr. April Robbins (National Institute of Arthritis, Diabetes, and Digestive and Kidney Diseases) for the CHO cell lines. We also thank Dr. Robbins, Drs.

Ira Mellman and Ari Helenius (Yale University), Dr. Mark Marsh (Institute of Cancer Research, Chester Beatty Laboratories), and Dr. Tim McGraw (Columbia University) for helpful discussions.

D. J. Yamashiro was supported by the Institutional Training grant GM-07827-05 and the Medical Scientist Training grant 5T32 GM-07308 from the National Institutes of Health. This work was supported in part by grant DK-27083 from the National Institutes of Health.

Received for publication 13 May 1987 and in final form 18 August 1987.

References

1. Basu, S. K., J. L. Goldstein, and M. S. Brown. 1978. Characterization of the low density lipoprotein receptor in membranes prepared from human fibroblasts. *J. Biol. Chem.* 253:3852–3856.
2. Brown, M. S., R. G. W. Anderson, and J. L. Goldstein. 1983. Recycling receptors: the roundtrip itinerary of migrant membrane proteins. *Cell.* 32:663–667.
3. Dautry-Varsat, A., A. Ciechanover, and H. F. Lodish. 1983. pH and the recycling of transferrin during receptor-mediated endocytosis. *Proc. Natl. Acad. Sci. USA.* 80:2258–2262.
4. Dorland, R. B., J. L. Middlebrook, and S. H. Leppla. 1979. Receptor-mediated internalization and degradation of diphtheria toxin by monkey kidney cells. *J. Biol. Chem.* 254:11337–11342.
5. Draper, R. K., and M. I. Simon. 1980. The entry of diphtheria toxin into the mammalian cell cytoplasm: evidence for lysosomal involvement. *J. Cell Biol.* 87:849–854.
6. Geuze, H. J., J. W. Slot, G. J. A. M. Strous, H. F. Lodish, and A. F. Schwartz. 1983. Intracellular site of asialoglycoprotein receptor-ligand uncoupling: double-label immunoelectron microscopy during receptor-mediated endocytosis. *Cell.* 32:277–287.
7. Geuze, H. J., J. W. Slot, and A. L. Schwartz. 1987. Membranes of sorting organelles display lateral heterogeneity in receptor distribution. *J. Cell Biol.* 104:1715–1723.
8. Gonzalex-Noriega, A., J. H. Grubb, V. Talkad, and W. S. Sly. 1980. Chloroquine inhibits lysosomal enzyme pinocytosis and enhances lysosomal enzyme secretion by impairing receptor recycling. *J. Cell Biol.* 85:839–852.
9. Helenius, A., I. Mellman, D. Wall, and A. Hubbard. 1983. Endosomes. *Trends Biochem. Sci.* 8:245–250.
10. Horwitz, M. A., and F. R. Maxfield. 1984. *Legionella pneumophila* inhibits acidification of its phagosome in human monocytes. *J. Cell Biol.* 99:1936–1943.
11. Hudson, T. H., and D. M. Neville, Jr. 1985. Quantal entry of diphtheria toxin to the cytosol. *J. Biol. Chem.* 260:2675–2680.
12. Kielian, M. C., M. Marsh, and A. Helenius. 1986. Kinetics of endosome acidification detected by mutant and wild type Semliki Forest virus. *EMBO (Eur. Mol. Biol. Organ. J.)* 5:3103–3109.
13. Klausner, R. D., J. van Renswoude, C. Kempf, K. Rao, J. L. Bateman, and A. R. Robbins. 1984. Failure to release iron from transferrin in a Chinese hamster ovary cell mutant pleiotrophically defective in endocytosis. *J. Cell Biol.* 98:1098–1101.
14. Leroy, J. G., M. W. Ho, M. C. MacBrinn, L. Zielke, J. Jacob, and J. S. O'Brien. 1972. I-Cell disease: biochemical studies. *Pediatr. Res.* 6: 732–757.
15. Lestas, A. N. 1976. The effect of pH upon human transferrin: selective labelling of the two iron-binding sites. *Br. J. Haematol.* 32:341–450.
16. Marsh, M., E. Bolzau, and A. Helenius. 1983. Penetration of Semliki forest virus from acidic prelysosomal vacuoles. *Cell.* 32:931–940.
17. Maxfield, F. R. 1982. Weak bases and ionophores rapidly and reversibly raise the pH of endocytic vesicles in cultured mouse fibroblasts. *J. Cell Biol.* 95:676–681.
18. Maxfield, F. R. 1985. Acidification of endocytic vesicles and lysosomes. *In* Endocytosis. I. Pastan and M. C. Willingham, editors. Plenum Publishing Corp., New York. 235–257.
19. McGraw, T. E., L. Greenfield, and F. R. Maxfield. 1987. Functional expression of the human transferrin receptor cDNA in Chinese hamster ovary cells deficient in endogenous transferrin receptor. *J. Cell Biol.* 105:207–214.
20. Mellman, I., R. Fuchs, and A. Helenius. 1986. Acidification of the endocytic and exocytic pathways. *Annu. Rev. Biochem.* 55:663–700.
21. Moss, D. W. 1983. Acid phosphatases. *In* Methods of Enzymatic Analysis. Vol. IV, 3rd ed. H. V. Bergmeyer, editor. Verlag Chemie, Weinheim. 92–106.
22. Mueller, S. C., and A. L. Hubbard. 1986. Receptor-mediated endocytosis of asialoglycoproteins by rat hepatocytes: receptor-positive and receptor-negative endosomes. *J. Cell Biol.* 102:932–942.
23. Olsnes, S., and K. Sandvig. 1985. Entry of polypeptide toxins into animal cells. *In* Endocytosis. I. Pastan and M. C. Willingham, editors. Plenum Publishing Corp., New York. 195–234.
24. Pastan, I., and M. C. Willingham. 1983. Receptor-mediated endocytosis: coated pits, receptosomes and the Golgi. *Trends Biochem. Sci.* 8: 250–254.
25. Poole, B., and S. Ohkuma. 1981. Effect of weak bases on the intralysosomal pH of mouse peritoneal macrophages. *J. Cell Biol.* 90: 665–669.
26. Princiotto, J. V., and E. J. Zapolski. 1975. Difference between the two iron-binding sites of transferrin. *Nature (Lond.)* 255:87–88.
27. Robbins, A. R., S. S. Peng, and J. L. Marshall. 1983. Mutant Chinese hamster ovary cells pleiotropically defective in receptor-mediated endocytosis. *J. Cell Biol.* 96:1064–1071.
28. Robbins, A. R., C. Oliver, J. L. Bateman, S. S. Krag, C. J. Galloway, and I. Mellman. 1984. A single mutation in Chinese hamster ovary cells impairs both Golgi and endosomal function. *J. Cell Biol.* 99:1296–1308.
29. Roederer, M., R. Bowser, and R. F. Murphy. 1987. Kinetics and temperature dependence of exposure of endocytosed material to proteolytic enzymes and low pH: evidence for a maturation model for the formation of lysosomes. *J. Cell. Physiol.* 131:200–209.
30. Roff, C. F., R. Fuchs, I. Mellman, and A. R. Robbins. 1986. Chinese hamster ovary cell mutants with temperature-sensitive defects in endocytosis. I. Loss of function on shifting to the nonpermissive temperature. *J. Cell. Biol.* 103:2283–2297.
31. Sandvig, K., and S. Olsnes. 1980. Diphtheria toxin entry into cells is facilitated by low pH. *J. Cell Biol.* 87:828–832.
32. Sipe, D. M., and R. F. Murphy. 1987. High resolution kinetics of transferrin acidification in Balb/c 3T3 cells: exposure to pH 6 followed by temperature-sensitive alkalinization during recycling. *Proc. Natl. Acad. Sci. USA.* 84:7119–7123.
33. Steinman, R. M., I. S. Mellman, W. A. Muller, and Z. A. Cohn. 1983. Endocytosis and the recycling of plasma membrane. *J. Cell Biol.* 96: 1–27.
34. Storrie, B., R. R. Pool, Jr., M. Sachdeva, K. M. Maurey, and C. Oliver. 1984. Evidence for both prelysosomal and lysosomal intermediates in endocytic pathways. *J. Cell. Biol.* 98:108–115.
35. Tanasugarn, L., P. McNeil, G. T. Reynolds, and D. L. Taylor. 1984. Microspectrofluorometry by digital image processing: measurement of cytoplasmic pH. *J. Cell Biol.* 98:717–724.
36. Tycko, B., and F. R. Maxfield. 1982. Rapid acidification of endocytic vesicles containing α_2-macroglobulin. *Cell.* 28:643–651.
37. Tycko, B., C. H. Keith, and F. R. Maxfield. 1983. Rapid acidification of endocytic vesicles containing asialoglycoprotein in cells of a human hepatoma line. *J. Cell. Biol.* 97:1762–1776.
38. Wolkoff, A. W., R. D. Klausner, G. Ashwell, and J. Harford. 1984. Intracellular segregation of asialoglycoproteins and their receptor: a prelysosomal event subsequent to dissociation of the ligand-receptor complex. *J. Cell Biol.* 98:375–381.
39. Yamashiro, D. J., and F. R. Maxfield. 1984. Acidification of endocytic compartments and the intracellular pathways of ligands and receptors. *J. Cell. Biochem.* 26:231–246.
40. Yamashiro, D. J., and F. R. Maxfield. 1987. Kinetics of endosome acidification in mutant and wild-type Chinese hamster ovary cells. *J. Cell Biol.* 105:2713–2721.
41. Yamashiro, D. J., B. Tycko, S. R. Fluss, and F. R. Maxfield. 1984. Segregation of transferrin to a mildly acidic (pH 6.5) para-Golgi compartment in the recycling pathway. *Cell.* 37:789–800.